Photochemistry and Photobiology

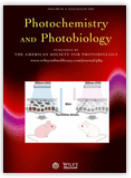

Volume 96, Issue 4

Pages: 729-950
July/August 2020

‹ Previous Issue

GO TO SECTION

Export Citation(s)

Issue Information

Free Access

Issue Information

Pages: 729-730 | First Published: 27 July 2020

First Page | PDF | Request permissions

Rapid Communications

Free Access

Estimated Inactivation of Coronaviruses by Solar Radiation With Special Reference to COVID-19

Jose-Luis Sagripanti, C. David Lytle

Pages: 731-737 | First Published: 05 June 2020

The ultraviolet B component of sunlight has the potential to significantly lower the infectivity of the SARS-CoV-2 virus that causes COVID-19. This effect varies in different geographic locations, being greater at lower latitudes during the summer. In addition, comparison with the seasonal incidence of influenza suggests that there should be an even greater seasonal effect on COVID-19 occurrence. Thus, indoor quarantining or in-house lock-down of healthy individuals during the summer should be discouraged.

Abstract | Full text | PDF | References | Request permissions

Phototherapy May be a Useful Adjuvant Therapy for Retractable Chronic Spontaneous Urticaria: A Systematic Review

Ji Yeon Hong, Myung Hwa Kim, Ji Hyun Lee, Hye Sung Han, Seong Jun Seo, Kui Young Park, Young Min Park

Pages: 738-740 | First Published: 06 March 2020

Chronic spontaneous urticaria (CSU) is highly prevalent and often refractory to the conventional treatment options. In this systematic review, it was observed that NBUVB could be an effective

Submit an Article

Browse free sample issue

Get content alerts

Subscribe to this journal

Published on behalf of the American Society for Photobiology

More from this journal

- Professional Opportunities
- NIH Public Access Mandate
- End Note Reference Style
- Special Issues and Symposia-in-Print
- Virtual Issue on Photosensory Biology
- Awards
- Virtual Issue: Type I and II Photosensitized Oxidation in Chemistry and Biology
- PHP Virtual Issue: International Congress on Photobiology
- Journal Information
- Jobs

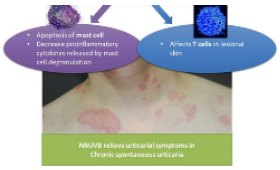

complementary treatment modality to manage refractory CSU. The efficacy of NBUVB to relieve urticarial symptoms may be explained by two mechanisms. First, NBUVB is proposed to induce apoptosis of dermal mast cells and decrease the production of proinflammatory cytokines released by mast cell degranulation. Second, UVB may primarily affect the T cells in lesional skin, which probably plays a key role in the pathogenesis of urticaria.

Abstract | Full text | PDF | References | Request permissions

Invited Reviews

Free Access

Upconversion Nanoparticle-Assisted Photopolymerization

Ke Wang, Jhair Peña, Jinfeng Xing

Pages: 741-749 | First Published: 01 March 2020

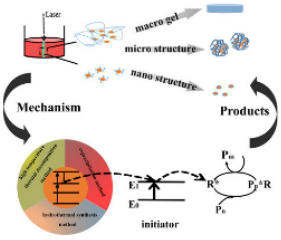

The upconversion nanoparticles (UCNPs) absorb two or more low-energy photons at near-infrared wavelength to emit high-energy photons at UV/vis wavelength to excite the initiator to generate free radicals, which induce monomers to polymerize to form various nano/micro structures or macro gels.

Abstract | Full text | PDF | References | Request permissions

Free Access

Two Distinct Photoprocesses in Cyanobacterial Bilin Pigments: Energy Migration in Light-Harvesting Phycobiliproteins *versus* Photoisomerization in Phytochromes

Vitaly A. Sineshchekov, Olga D. Bekasova

Pages: 750-767 | First Published: 23 December 2019

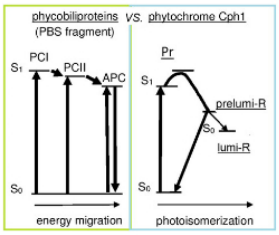

Cyanobacterial phycobiliproteins and phytochromes (Cph1 as a model), with open-chain tetrapyrroles as chromophores, differ by photophysical and photochemical properties. The phycobiliproteins are highly fluorescent, which is a prerequisite for energy transfer, whereas the phytochromes are practically nonfluorescent and possess a capacity for photoisomerization. In the phycobiliproteins, this is provided by "freezing" of chromophore torsional relaxations by its fixation by the apoprotein. In the case of the phytochromes, on the contrary, the chromophore–apoprotein interaction leaves room for torsional movements and the photo-induced flip of the D-ring. These properties make the phycobiliproteins highly efficient photosynthetic light-harvesters and the phytochromes—photosensors.

Abstract | Full text | PDF | References | Request permissions

Free Access

Chaetopterus variopedatus Bioluminescence: A Review of Light Emission within a Species Complex

Jeremy D. Mirza, Álvaro E. Migotto, Ilia V. Yampolsky, Gabriela V. de Moraes, Aleksandra S. Tsarkova, Anderson G. Oliveira

Pages: 768-778 | First Published: 03 February 2020

Chaetopterus variopedatus transferred from its burrow to a glass tube and photographed with a digital camera (Sony A7). Under natural light, and in the dark with an ISO of 60000, to show bioluminescent regions, following stimulation by addition of 1 M KCl.

Abstract | Full text | PDF | References | Request permissions

Free Access

Materials Science Challenges in Skin UV Protection: A Review

Orielia Pria Egambaram, Sreejarani Kesavan Pillai, Suprakas Sinha Ray

Pages: 779-797 | First Published: 30 December 2019

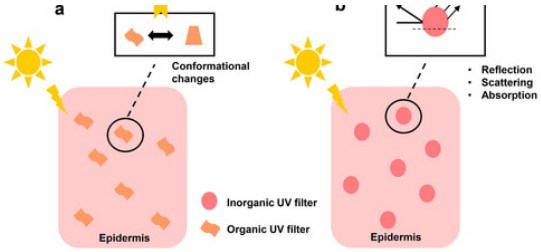

The sun is a vital component of our daily lives, from food to personal health and well-being. Lack of sun exposure has detrimental effects on our health. Likewise, overexposure to sun leaves us with long-term negative effects which may ultimately be worse than those caused by the lack of sun exposure. Sunscreen agents have been used for many years. Over time, UV filters have changed in hopes of being more effective; unfortunately, this has come at the cost of posing a risk to the consumer's health and environment thus raising the question, is it really worthwhile using sunscreen?

Abstract | Full text | PDF | References | Request permissions

Research Articles

Photolysis of 3-(1-acyl-5-aryl-3-pyrazolinyl)coumarins—Effective Fluorescence Decay

Valerii F. Traven, Dmitriy A. Cheptsov, Zarina Z. Mamirgova, Natalya P. Solovjova, Vyacheslav M. Martynenko, Sergei M. Dolotov, Michail M. Krayushkin, Ivan V. Ivanov

Pages: 798-804 | First Published: 04 January 2020

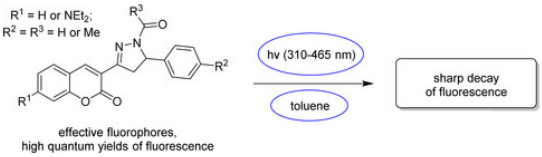

The photophysical characteristics of the new 3-(1-acyl-5-aryl-3-pyrazolinyl)coumarins were measured. These compounds are effective fluorophores and possess high quantum yields of fluorescence. 3-(1-Acyl-5-aryl-3-pyrazolinyl)coumarins undergo easy photolysis with a sharp decay of fluorescence. These results may be of interest for the creation of new carriers for optical recording of information.

Abstract | Full text | PDF | References | Request permissions

Theoretical Study of the Wavelength Selection for the Photocleavage of Coumarin-caged D-luciferin

Junko Usukura, Miyabi Hiyama, Maki Kurata, Yuji Hazama, Xing-Ping Qiu, Francoise M. Winnik, Hidefumi Akiyama, Nobuaki Koga

Pages: 805-814 | First Published: 06 January 2020

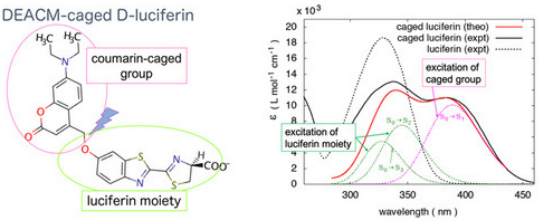

The equilibrium structures and optical properties of the photolabile caged luciferin (7-diethylaminocoumarin-4-yl)methyl caged D-luciferin (DEACM-caged D-luciferin) in aqueous solution were investigated via quantum chemical calculations. We obtained a theoretical UV/Vis spectrum of DEACM-caged D-luciferin, which has two main bands of shape nearly identical to the experimental UV/Vis spectrum. The absorption bands centered ~ 384 and 339 nm were attributed to the electronic excitations of the caged group and the luciferin moiety, respectively. DEACM-caged D-luciferin can be excited in the caged group only by light of wavelength ranging from 400 to 430 nm, which is in the long-wavelength tail of the 384 nm band.

Abstract | Full text | PDF | References | Request permissions

Experimental and Theoretical Study of the Stability of the Complex Fisetin–Cu(II) and A Comparative Study of Free Ligand and Complex Interaction with Molecular Singlet Oxygen

Vanesa A. Muñoz, Frida C. D. Dimarco Palencia, Matias I. Sancho, Sandra Miskoski, Norman A. García, Gabriela V. Ferrari, María Paulina Montaña

Pages: 815-825 | First Published: 07 January 2020

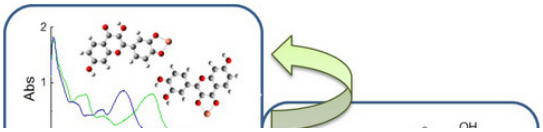

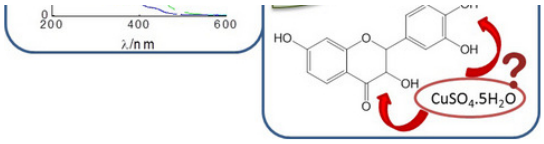

Flavonoids can exert protection against oxidative damage caused by reactive oxygen species, and this biological activity could be affected by chelation with metallic ions. The stoichiometry and the apparent formation constant of the fisetin–Cu(II) complex were determined. The molecular structure of fisetin shows two possible chelation sites. A molecular modeling analysis of fisetin and its complex was performed to study spectroscopic properties and compared with experimental data.

Abstract | Full text | PDF | References | Request permissions

Open Access

Age-Related Absorption of the Human Lens in the Near-Ultraviolet Range

Viktor Pajer, Ferenc Rárosi, Lajos Kolozsvári, Béla Hopp, Antal Nógrádi

Pages: 826-833 | First Published: 19 December 2019

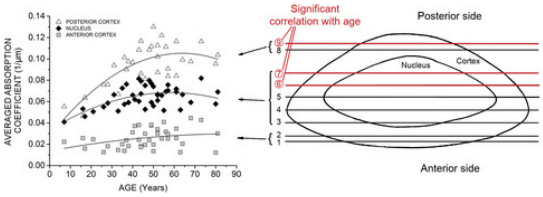

The UV absorbance of nine samples, derived from different parts of the lens, was determined. The absorbance of the anterior and posterior capsules was measured separately. The absorption coefficients were calculated from the absorbance. Older lenses have a more efficient anatomically independent UV absorption capacity than the younger samples. Statistical analysis of the values taken at 280 nm and at 360-nm wavelengths shows that correlation between the absorption coefficients and age can be found only in the case of the posterior layers. Posterior capsules have higher absorption coefficient than the anterior ones but no significant changes were found.

Abstract | Full text | PDF | References | Request permissions

Anionic Conjugated Polyelectrolytes for FRET-based Imaging of Cellular Membrane Potential

Okhil K. Nag, Ji-Eun Jeong, Van Sang Le, Eunkeu Oh, Han Young Woo, James B. Delehanty

Pages: 834-844 | First Published: 21 February 2020

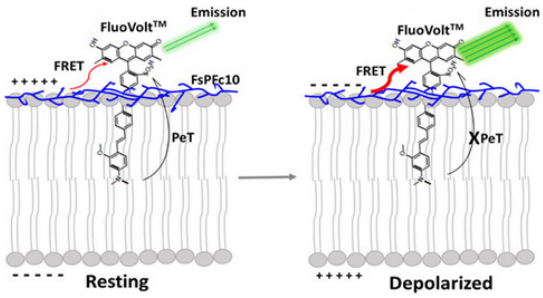

Förster resonance energy transfer (FRET)-based imaging of membrane potential using a conjugated polymer (FsPFc10) donor and FluoVolt™ acceptor. Depolarization of membrane potential results in decreased rate of photoinduced electron transfer (PeT) in FluoVolt™. This results in enhanced emission from FluoVolt™ by efficient light harvesting and energy transfer from the FsPFc10 donor.

Abstract | Full text | PDF | References | Request permissions

Spatial and Temporal Bioactive Compound Contents and Chlorophyll Fluorescence of Kale (*Brassica oleracea* L.) Under UV-B Exposure Near Harvest Time in Controlled Environments

Hyo In Yoon, Damin Kim, Jung Eek Son

Pages: 845-852 | First Published: 27 February 2020

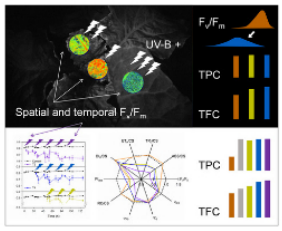

The spatial effect of UV-B irradiation on plants was examined to enhance the secondary metabolite content. The study demonstrated the spatial and temporal effects of UV-B stress on chlorophyll fluorescence kinetics and bioactive compound accumulation in kale. In both aspects, the more UV-B exposure, the lower the F_v/F_m value and the higher the concentration in total flavonoid compound. Most of the fluorescence transient parameters decreased with increasing UV-B stress period. When exposed to UV-B radiation for two days before harvest, the highest accumulation of total phenolic and flavonoid compounds was expected in the entire plant

plant.

Abstract | Full text | PDF | References | Request permissions

Open Access

Long-term Effects of 222-nm ultraviolet radiation C Sterilizing Lamps on Mice Susceptible to Ultraviolet Radiation

Nozomi Yamano, Makoto Kunisada, Sachiko Kaidzu, Kazunobu Sugihara, Aiko Nishiaki-Sawada, Hiroyuki Ohashi, Ai Yoshioka, Tatsushi Igarashi, Akihiro Ohira, Masaki Tanito, Chikako Nishigori

Pages: 853-862 | First Published: 29 March 2020

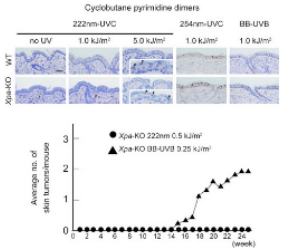

222-nm UVC have been reported to exert sterilizing ability comparable to that of 254-nm UVC without producing cyclobutane pyrimidine dimers (CPDs), the major DNA lesions caused by UV. We investigated the long-term effects of 222-nm UVC on skin using *Xpa*-knockout mice, a highly photocarcinogenic phenotype mice. CPDs formation was recognized only in uppermost layer of epidermis with 222-nm UVC exposure. No tumors were observed in *Xpa*-knockout mice and wild-type mice by repetitive irradiation with 222-nm UVC. These data reveal that 222-nm UVC lamps can be safely used for sterilizing human skin as far as the perspective of nonmelanoma skin cancer development.

Abstract | Full text | PDF | References | Request permissions

Tranexamic Acid Cream Protects Ultraviolet B-induced Photoaging in Balb/c Mice Skin by Increasing Mitochondrial Markers: Changes Lead to Improvement of Histological Appearance

Fransiska Eltania, Ronny Lesmana, Sunaryati Sudigdoadi, Sudigdoadi Sudigdoadi, Astrid Feinisa Khairani, Hanna Goenawan, Andrew Citrawan, Rina Armina Yuniarti, Roro Wahyudianingsih, Julia Windi Gunadi, Unang Supratman

Pages: 863-869 | First Published: 01 December 2019

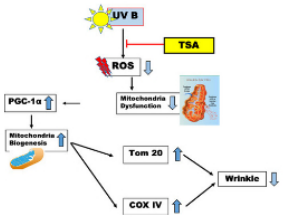

Tranexamic acid (TSA) is used as an antiaging treatment for reducing melasma and wrinkles. One mechanism for wrinkle formation is mitochondrial damage. We investigated how the application of TSA cream affects mitochondrial protein levels in mouse skin exposed to UVB (PGC1α, Tom20, COX IV). Thirty mice (Balb/C, male) were divided into five groups (negative control—no UVB, no TSA; positive control —UVB, no TSA; TSA 3%+UVB; TSA 4%+UVB; and TSA 5%+UVB). H&E staining revealed that TSA treatment increased mitochondrial marker levels and epidermal thickness while decreasing dermal elastosis for all the treatment groups.

Abstract | Full text | PDF | References | Request permissions

Bucillamine Inhibits UVB-Induced MAPK Activation and Apoptosis in Human HaCaT Keratinocytes and SKH-1 Hairless Mouse Skin

Adil Anwar, Hiba Anwar, Takeshi Yamauchi, Ryan Tseng, Rajesh Agarwal, Lawrence D Horwitz, Zili Zhai, Mayumi Fujita

Pages: 870-876 | First Published: 19 February 2020

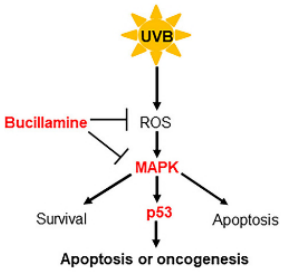

Bucillamine, a cysteine derivative with antioxidant and anti-inflammatory capacity, protects against UVB-induced apoptosis via inhibition of MAPK activation in human HaCaT keratinocytes and SKH-1 hairless mouse skin.

Abstract | Full text | PDF | References | Request permissions

Dose–Response and Temperature Dependence of the Mortality of Spider Mite and Predatory Mite Eggs Caused by Daily Nighttime Ultraviolet-B Irradiation

Lifeng Yuan, Masahiro Osakabe

Pages: 877-882 | First Published: 30 December 2019

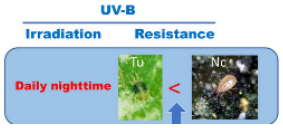

Daily nighttime UV-B irradiation is used for spider mite control in strawberry greenhouse in Japan. It has been known that UV-B resistance is higher in spider mites (Tu) than phytoseiid mites (natural enemy; Nc) under a single irradiation. However, it reversed under daily nighttime irradiation, being

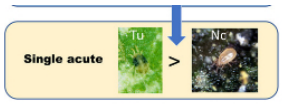

reversed under daily nighttime irradiation, being advantageous to the combined use of phytoseiid mites with UV-B in greenhouse. Our study also shows clear temperature dependence of the UV-B damage to this prey–predator system; larger and smaller at lower and higher temperatures, respectively.

Abstract | Full text | PDF | References | Request permissions

Open Access

First Report on Photodynamic Inactivation of Archaea Including a Novel Method for High-Throughput Reduction Measurement

Daniel B. Eckl, Harald Huber, Wolfgang Bäumler

Pages: 883-889 | First Published: 19 February 2020

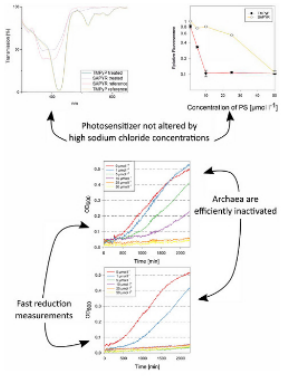

To date, no report is available of photodynamic inactivation (PDI) of any archaeal cells. Two photosensitizers (SAPYR and TMPyP) were used to investigate PDI of *Halobacterium salinarum*. A novel high-throughput method that allows high sample throughput was tested to evaluate microbial reduction. Due to the high salt content of the culture medium, the properties of photosensitizers were analyzed *via* spectroscopy and fluorescence-based assays. The presented results indicate that PDI is working even in high salt environments. Either photosensitizer inactivated the archaeal cells with a reduction of 99.9% at least.

Abstract | Full text | PDF | References | Request permissions

Pretreatment of Root Canal with Photodynamic Therapy Facilitates Adhesion, Viability and Differentiation of Stem Cells of the Apical Papilla

Yijun Li, Huan Ge, Lixuan Wu, Lishan Lei, Yanhuang Wang, Shan Jiang, Zhiyu Cai, Xiaojing Huang

Pages: 890-896 | First Published: 27 February 2020

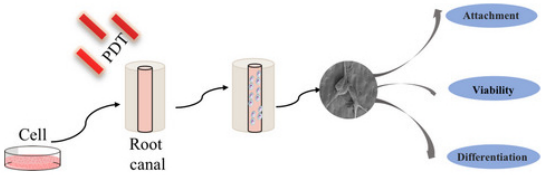

Under the limitation of this study, PDT could facilitate cell adhesion, viability and differentiation of SCAP without reducing microhardness and smear layer removal of root canal wall.

Abstract | Full text | PDF | References | Request permissions

Recapitulation of Hypoxic Tumor–stroma Microenvironment to Study Photodynamic Therapy Implications

María Julia Lamberti, Ana Belén Morales Vasconsuelo, María Gracia Ferrara, Natalia Belén Rumie Vittar

Pages: 897-905 | First Published: 03 February 2020

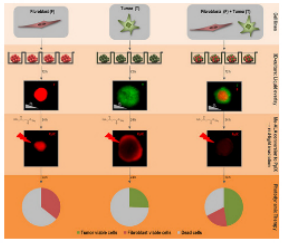

Tumor GFP + and fibroblast RFP + cells were cultured alone (homotypic spheroids) or as a 1:1 mixed suspension (heterotypic spheroids) using liquid-overlay method. Heterotypicspheroids demonstrated a hybrid distribution of both cell types where relative localization of fibroblasts in the hypoxic region was observed. To characterize the hypoxic stromal/tumor metabolism of Me-ALA, homotypic spheroids were incubated with the photosensitizer PpIX (24 h); preferential stromal PpIX generation was observed. Photosensitizer production was inhibited in mixed spheroids. The impact of PDT on homo and heterotypic spheroids was identified by exposing Me-ALA-incubated 3D cultures to red-light irradiation. The presence of fibroblasts increased tumor photoresistance in heterotypic spheroid.

Abstract | Full text | PDF | References | Request permissions

Effect of Photobiomodulation on C2C12 Myoblasts Cultivated in M1 Macrophage-conditioned Media

Tainá Caroline dos Santos, Kaline de Brito Sousa, Lucas Andreo, Andreia Martinelli, Maria Fernanda Setubal Destro Rodrigues, Sandra Kalil Bussadori,

Kristianne Porta Santos Fernandes, Raquel Agnelli Mesquita-Ferrari

Pages: 906-916 | First Published: 06 January 2020

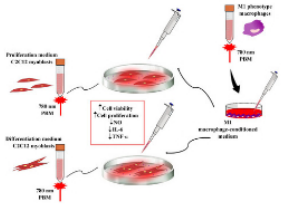

The muscle repair is dependent on moderate levels of mediators secreted from macrophages. This study investigated the effects of photobiomodulation (PBM: 780 nm) on undifferentiated and differentiation-induced C2C12 myoblasts cultivated in an activated M1 macrophage-conditioned medium submitted to irradiation with the same parameters. Results showed that the increase synthesis of proinflammatory markers could inhibit the fusion of myoblasts. PBM was able to modulate the viability and proliferation of myoblasts and promoted reductions in nitric oxide, IL-6 and TNF-α synthesis.

Abstract | Full text | PDF | References | Request permissions

Open Access

Photoprotection by Workwear: Ultraviolet Protection Factors for Artificial Radiation from Welding Arcs

Stefan Bauer

Pages: 917-925 | First Published: 16 December 2019

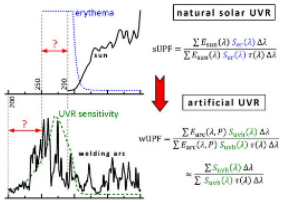

Ultraviolet protection factors (UPF) for clothing are based on the solar ultraviolet radiation (UVR) spectrum in conjunction with the CIE erythema weighting function and consider the textile's UVR transmittance for wavelengths above 290 nm. However, workwear exposed to welding arcs that emit significant UVR at shorter wavelengths has to fulfill additional textile photoprotection criteria. Therefore, a welding UPF (wUPF) is proposed taking into account the welding arc's full UVR emission spectrum and ICNIRP's relative spectral effectiveness for UVR hazards. Analyzing the new protection factor regarding welding power, technique and welded material led to a reduced wUPF equation.

Abstract | Full text | PDF | References | Request permissions

The Simulated Ocular and Whole-Body Distribution of Natural Sunlight to Kiteboarders: A High-Risk Case of UVR Exposure for Athletes Utilizing Water Surfaces in Sport

Nathan J. Downs, Alfio V. Parisi, Peter W. Schouten, Damien P. Igoe, Guillermo De Castro-Maqueda

Pages: 926-935 | First Published: 28 December 2019

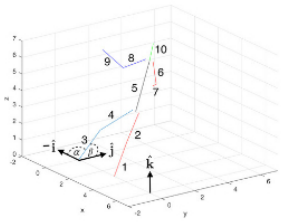

The research measures the expected body surface exposure of solar UVR to kiteboarders. Measured exposures are presented for 17 body sites. The expected body orientation is derived from video vector analysis of kiteboarders filmed in motion. A novel methodology for deriving UVR exposure in aquatic sports is presented with positive implications for skin cancer prevention, policy development, consumer education and sun protection awareness.

Abstract | Full text | PDF | References | Request permissions

Research Notes

Effects of Temperature on The UV-B Sensitivity of Toxic Cyanobacteria *Microcystis aeruginosa* CS558 and *Anabaena circinalis* CS537

Md Ashraful Islam, John Beardall

Pages: 936-940 | First Published: 06 January 2020

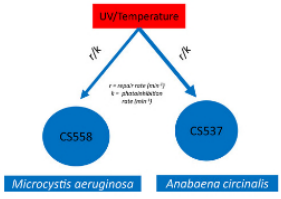

The interactive effects of temperature and UV-B on two species of toxic cyanobacteria *Microcystis aeruginosa* and *Anabaena circinalis* were studied. Differences between species in terms of repair (*r*) and photodamage (*k*) were observed. In both species, repair rates and the ratio of *r*:*k* were higher at 30 °C. However, the percent inhibition of effective quantum yield by UV-B was greater in *A. circinalis* than in *M. aeruginosa* as the *r*:*k* was lower *A. circinalis*. It could be concluded that temperature may influence growth and bloom formation of cyanobacteria and different species may respond differently to UVB and temperature interactions.

Abstract | Full text | PDF | References | Request permissions

Skin Cancer Awareness Among 1 271 Black Africans in South Africa

Caradee Y. Wright, Melissa Wallace, Preethi Mistri, Bianca Wernecke, Thandi Kapwata

Pages: 941-942 | First Published: 16 December 2019

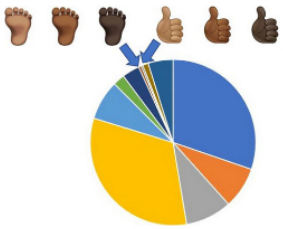

We interviewed 1271 participants with deeply pigmented skin. Ninety percent of all participants had never checked their skin for signs or symptoms of skin cancer. Palms of hands and soles of feet were the least recognised sites for skin cancer development despite these anatomic sites being most common for the development of acral lentiginous melanoma in people with deeply pigmented skin. While it is known that skin cancer can affect Black Africans on anatomic sites never exposed to sunlight, our results suggest a need for targeted skin cancer awareness on identification, screening and early detection.

Abstract | Full text | PDF | References | Request permissions

Drivers for Sun Protection in Black South Africans

Brian Diffey, Melissa Wallace, Preethi Mistri, Bianca Wernecke, Caradee Y. Wright

Pages: 943-944 | First Published: 19 December 2019

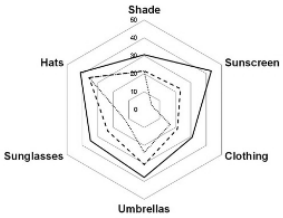

Sun protection use among individuals with deeply pigmented skin is not well understood. We analyzed 1271 participant responses from a survey among Black South Africans. The main driver for using sun protection was awareness of skin cancer. Different sun protection modalities were used by respondents and when categorized by Living Standard Measure groups in low (1–4; dotted line), intermediate (5–7; dashed line) and high (8–10; solid line) patterns emerged. Most striking was the difference in use of sunscreen among the high and low groups.

Abstract | Full text | PDF | References | Request permissions

Availability of hats that meet Australian sun-safety standards at a major Canberra shopping complex†

Vangelis George Kanellis, Alice Louise Kanellis

Pages: 945-948 | First Published: 03 March 2020

This study investigated the availability of sun-safe hats during a three-day cross-sectional survey in November 2019 by visiting every shop in a large multi-store shopping complex in the Australian Capital Territory, Australia. Wearing a sun-protective hat that meets defined photoprotective criteria, such as the 2017 Australian/New Zealand standard (AS/NZS 4399:2017), is an essential element of good sun-safe practice. Disappointingly, 69% of the hats for sale to adults and children did not meet the AS/NZS 4399:2017. Of the 9% of hats that had swing tags claiming an Ultraviolet Protection Factor of 50 (UPF-50), about half were not sun safe.

Abstract | Full text | PDF | References | Request permissions

Highlight Article

Harmless Effects of Sterilizing 222-nm far-UV Radiation on Mouse Skin and Eye Tissues

Jean Cadet

Pages: 949-950 | First Published: 11 June 2020

Abstract | Full text | PDF | References | Request permissions

Photochemistry and Photobiology, 20**, **: *–*

Tranexamic Acid Cream Protects Ultraviolet B-induced Photoaging in Balb/c Mice Skin by Increasing Mitochondrial Markers: Changes Lead to Improvement of Histological Appearance

Fransiska Eltania[1,2], Ronny Lesmana*[3,4,5], Sunaryati Sudigdoadi[2,6], Sudigdoadi Sudigdoadi[2], Astrid Feinisa Khairani[2,7], Hanna Goenawan[3,4], Andrew Citrawan[8], Rina Armina Yuniarti[9], Roro Wahyudianingsih[10], Julia Windi Gunadi[11] and Unang Supratman[5,12]

[1]Department of Pharmacology, Faculty of Medicine, Maranatha Christian University, Bandung, Indonesia
[2]Graduate Programme of Antiaging and Aesthetics Medicine, Faculty of Medicine, Universitas Padjadjaran, Bandung, Indonesia
[3]Physiology Division, Department of Biomedical Sciences, Faculty of Medicine, Universitas Padjajaran, Bandung, Indonesia
[4]Division of Biological Activity, Central Laboratory, Universitas Padjajaran, Bandung, Indonesia
[5]Center of Excellence in Higher Education for Pharmaceutical Care Innovation, Universitas Padjajaran, Bandung, Indonesia
[6]Microbiology Division, Department of Biomedical Sciences, Faculty of Medicine, Universitas Padjajaran, Bandung, Indonesia
[7]Division of Cell Biology, Department of Biomedical Sciences, Faculty of Medicine, Universitas Padjajaran, Bandung, Indonesia
[8]Luminos Aestethic Clinic, Telogorejo Hospital, Semarang, Indonesia
[9]Carissa Aestethic Clinic, Bandung, Indonesia
[10]Department of Pathology Anatomy, Faculty of Medicine, Maranatha Christian University, Bandung, Indonesia
[11]Department of Physiology, Faculty of Medicine, Maranatha Christian University, Bandung, Indonesia
[12]Department of Chemistry, Faculty of Mathematics and Natural Sciences, Universitas Padjadjaran, Jatinangor, Indonesia

Received 15 August 2019, accepted 2 November 2019, DOI: 10.1111/php.13189

ABSTRACT

Tranexamic acid (TSA) is widely used as an antiaging treatment for reducing melasma and wrinkles. There are various mechanisms for wrinkle formation, and one of them is due to damage of the mitochondria. Research on mitochondria in the skin is very limited, so we are interested to see the changes that occur after application of TSA cream. We explored the effect of TSA on mitochondrial protein levels (PGC1α, Tom20, COX IV), which had affected to skin histological structure. Thirty male, 6-week-old, Balb/C mice were divided into five groups (negative control, positive control, TSA 3%, TSA 4% and TSA 5%). After 10 days of acclimatization, four groups of mice were exposed to UVB light, of which three groups were given TSA cream for 10 weeks. The skin tissue was excised for protein and histological studies. H&E staining was performed for evaluating histological changes in epidermal thickness and dermal elastosis. TSA treatment on the mice skin increased mitochondrial marker levels and epidermal thickness while decreasing dermal elastosis for all the treatment groups. Topical application of TSA significantly increased mitochondrial biogenesis which may cause alteration in epidermal thickness and reduced dermal elastosis in the histology of mice skin.

INTRODUCTION

The skin is the most visible indicator of age in the aging process (1). Skin aging involves intrinsic and extrinsic factors. Photoaging can caused by extrinsic factors such as chronic UV B exposure (2). UVB increases the production of reactive oxygen species (ROS), which is responsible for oxidative damage to proteins, DNA, RNA and lipids, dysregulated pathways that modulate the inflammatory response and apoptosis (3). Excessively increased ROS causes accumulative damage to biological structures over time, which causes loss of cellular function and aging, especially mitochondria (4).

Mitochondria is an organelle that has a primary function as an energy producer through a series of oxidative phosphorylation processes or electron chain transport that occurs in the inner membrane of the mitochondria. Physiologically, this oxidative phosphorylation will produce ROS in mitochondria complexes I and III as side product, and therefore, mitochondria is responsible as the highest ROS producer in cells (5,6). Mitochondria has a risk of mutation because mitochondrial DNA (mtDNA) is located close to where ROS is produced in the inner membrane of the mitochondria. In addition, mtDNA does not have histones, so that mtDNA has a risk of up to 50 times of mutation compared with that of nucleus DNA (7,8). MtDNA is very important in carrying out mitochondrial function, in which accumulation of mtDNA mutations can cause mitochondrial dysfunction and plays a role in the aging process (9,10).

Aging induced mtDNA damage via many stimulators like radical ROS. Aging increases ROS production, and its process is similar to induction by UV radiation. ROS sporadically attacks

*Corresponding author email: ronny@unpad.ac.id (Ronny Lesmana)

cell DNA, and mtDNA is more susceptible to damage compared with nucleus DNA (11). MtDNA damage will affect mitochondrial biogenesis. Reduced biogenesis of mitochondria will affect the respiratory chain and disruption of the protein transport process from the cytoplasm to enter the mitochondria. Damage to the respiratory chain as a sign of mitochondrial dysfunction will result in more ROS and oxidative damage accumulation and produce faster mtDNA mutations and mtDNA damage (12). This is the basis of the "mitochondrial theory of aging," in which there is a vicious cycle due to the accumulation of oxidative damage from time to time as a result of increased ROS. MtDNA damage and mitochondrial dysfunction cause a decrease in cell function and a characteristic feature of aging that appears on the skin, one of which is wrinkles (6,9,13,14). Mitochondrial damage can be described by a decrease in the number of mitochondria described by Tom20 (15) and impaired mitochondrial function described by COX IV (16).

Chronic exposure to UVB rays can result in the formation of wrinkles on the skin. Wrinkles caused by photoaging give histological features of changes from the epidermal thickness, dermoepidermal junction and dermal elastosis as the gold standard of photoaging (17,18). There are many therapeutic modalities used for preventing wrinkles, one of those modalities is tranexamic acid (TSA), which has previously been widely used for the treatment of melasma (19,20). It had been reported that TSA oral administration can reduce the formation of wrinkles (21).

However, there is limited information about the effects of TSA on wrinkles and its potential mechanism on mitochondria. Our study will elaborate the effect of TSA cream on mitochondria, which plays a role in aging and its correlation to histological changes in the form of changes in epidermal thickness and dermal elastosis.

MATERIALS AND METHODS

Thirty, 6-week-old male *Mus musculus* species Balb/C strain, each weighing 20-30 g, were used in this experiment. Animals were housed in the animal house in Department of Pharmacology and Therapy, Universitas Padjadjaran, under a controlled room temperature and photoperiodicity of 12 h light/dark system. The animals were acclimatized for ten days prior to the study and randomly divided into five groups (n = 6 mice per group). The animals were assigned into five groups: negative control group (not exposed to UVB light and not treated with TSA cream), positive control group (exposed to UVB), TSA 3% group (exposed to UVB and treated with TSA 3% cream), TSA 4% group (exposed to UVB and treated with TSA 4% cream) and TSA 5% group (exposed to UVB and treated with TSA 5% cream) for ten weeks (Figure S1). All procedures were approved by Ethical Committee, Faculty of Medicine, Universitas Padjadjaran (Animal Ethics Number: 473/UN6.KEP/EC/2019).

UV irradiation. Mice were exposed to UV lamp (Kernel KN-4003, China) on their back skin with suberythemal doses of 166 mJ cm^{-2}, three times a week, for 10 weeks in all treatment groups and positive control. The total dose received by each mouse is 166mJ/ cm^2. UVB lighting used a holder, 3 cm apart from the skin of mice, and it was exposed to UVB for 100 s per session (Figure S2).

Tranexamic acid cream. TSA cream was applied on back skin of experimental animals of 0.1 g cm^{-2}. TSA cream was applied immediately after UVB exposure, once a day, for 10 weeks. The dose of TSA cream for the mice in this study was taken based on the dose of TSA cream for melasma in humans, which is between 3%, 4% and 5%. TSA cream with concentrations of 3%, 4% and 5% used in this study had the following basic cream compositions: water, butylene glycol, glycerin, PEG-6 esters almond oil, PEG-40 hydrogenated castor oil, phenoxyethanol, hydroxyethyl cellulose, PCA zinc and cetylpyridinium chloride.

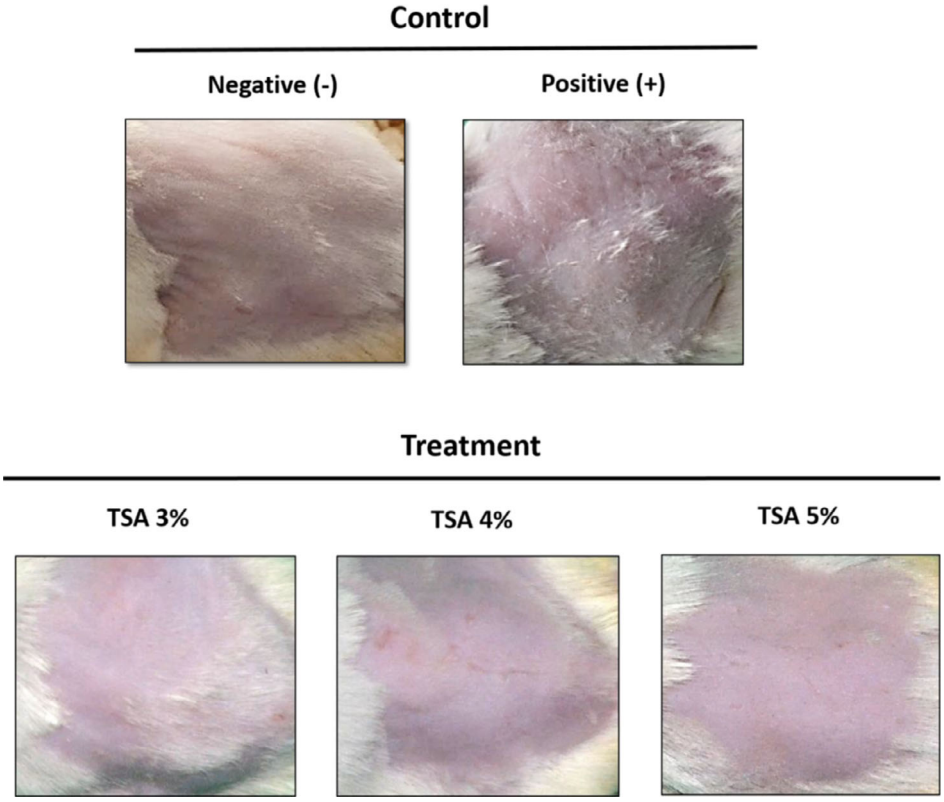

Figure 1. The morphological appearance of mice's skin in all groups after 10 weeks of UVB exposure with tranexamic acid application. There is wrinkle reduction found in all treatment groups (TSA 3%, 4% and 5%) compared with positive control group.

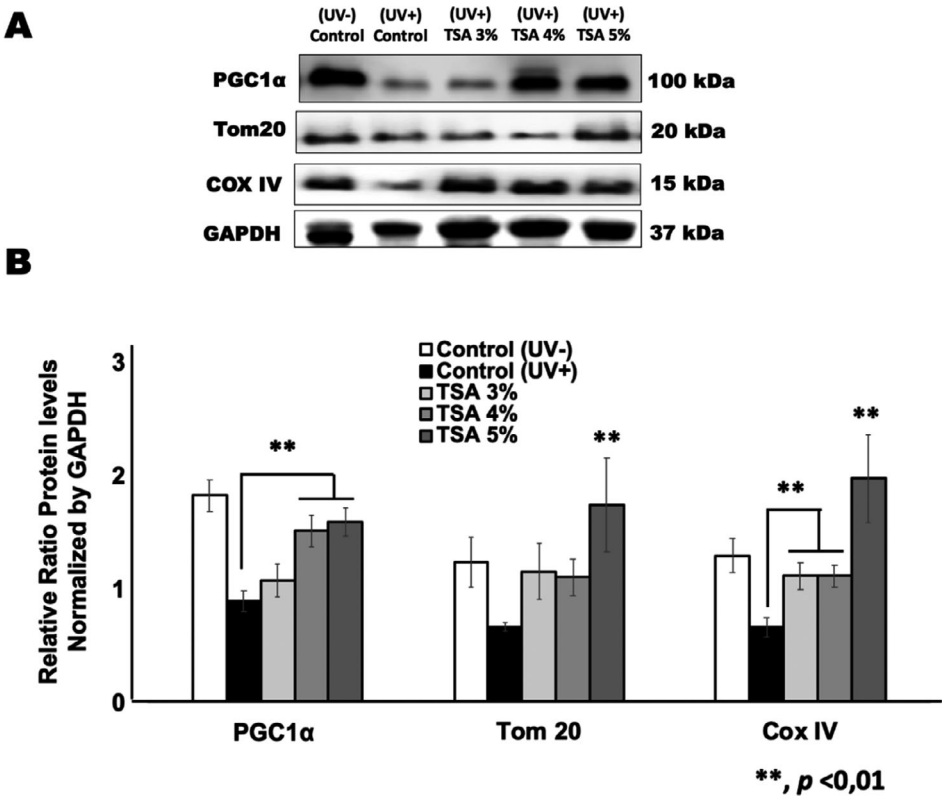

Figure 2. Evaluation of mitochondrial marker from Western blot after 10 weeks exposure of UVB with tranexamic acid cream application. (A) Exposure to UVB increased protein expression of PGC1α, Tom20 and COX IV in mice skin. (B) A significant increase in COX IV protein expression was found in TSA 3% and 5%, while Tom20 increased in TSA 5%, and PGC1α increased in all the treatments (TSA 3%, 4%, and 5%) compared with positive control. Data were presented as average mean ± standard error of mean (SEM) with $P < 0.05$ considered as significant (*) and $P < 0.01$ considered as very significant (**).

Skin sample collection. Twenty-four hours after the last UV exposure, mice were sacrificed CO_2 chamber. Skin samples were excised using sterile surgical blade and collected from gluteal area with size 3 × 3 cm^2. For Western blot sample, the skin was snap frozen using liquid nitrogen then stored at −80°C, and as for hematoxylin–eosin (HE) staining, the skin was stored in neutral buffer formalin in room temperature.

Protein extraction and Western blotting. Skin samples were lysed using RIPA lysis buffer (20 mM Tris-HCl pH 7.5; 150 mM NaCl; 1 mM Na2EDTA; 1 mM EGTA; 1% NP-40; 1% sodium deoxycholate; 2.5 mM sodium pyrophosphate; 1 mM β-glycerophosphate; 1 mM Na3VO4; and 1 μg mL^{-1} leupeptin) with 1 mM protease inhibitors cocktail (Sigma, Merck KGA, Darmstadt, Germany). The skin tissue lysates were centrifuged for 5 min at 15 000 ***g*** in temperature 4°C. Tissue lysates were added with sample buffer contained β-ME boiled for 5 min in 95°C. Equal amount of protein samples was resolved by SDS-PAGE gels and then transferred to nitrocellulose membranes. The nitrocellulose membranes were immunoblotted with anti-PGC-1α antibody (Cat no. PA5-38022), anti-Tom20 antibody (Cat no. sc-11415) and anti-COX IV antibody (Cat no. PA5-17511). The equality of protein loading was confirmed by probing blots with anti-GAPDH antibody (Cat no. AM4300). The secondary antibodies used were goat anti-mouse IgG secondary antibody HRP (sc-2005; Santa Cruz Biotechnology Inc., CA). The antigen–antibody complexes were detected by Western Sure ECL Substrate (LI-COR Biotechnology, Lincoln, NE) and visualized using LICOR Odyssey Western Blot Scanner (LI-COR Biotechnology). Densitometric analysis was performed using Image J software (NIH Image).

Histological examination by H&E staining. Five micrometer thick sections were collected from paraffin-embedded skin tissues. The sections were stained with hematoxylin (Cat no. GHS316; Sigma) and eosin solution (Cat no. HT110116; Sigma). H&E staining was performed as follows: hematoxylin staining for 10 min, water rinse for 10 min, eosin staining for 2 min, decoloring in 90% ethanol for 5 min, 95 % ethanol for 5 min and clearing in xylene solution for 5 min. After mounting, the tissues were observed by light microscopy Leica MD500. Histopathologic review was performed using Leica Application Suite E2 V2.0.0 for Windows (Carl Zeiss, German). Histological examination of the skin tissue was reviewed by a single expert anatomy pathologist (RW) who was blinded to all other features of the samples characteristics. All samples were evaluated for measuring epidermal thickness and dermal elastosis. Epidermal thickness was examined by measuring epidermal length from stratum corneum to stratum basale in six fields with 400-fold magnification (×400), representing the epidermal thickness, and then, the mean was calculated for each sample. Dermal elastosis was determined based on elastic fibers changes in skin tissue with 100-fold magnification (×100). Changes in elastin fibers were scored based on the Kligman score as follows: 0 thin and slightly wavy; +1 thin and simple increase in number; +2 thickened and numerous; +3 thickened, curling and dense; and + 4 almost complete replacement of the dermis by a dense tangle of thickened, amorphous masses (17). This score is modified into 3 degrees: 0 and + 1 as mild; +2 as moderate; and + 3 and + 4 as severe degrees (18,22).

Statistical analysis. Quantitative values were determined in at least three independent experiments and expressed as means ± standard error of mean (SEM). A statistical comparison of PGC1α, Tom20, COX IV, epidermal thickness and dermal elastosis in all groups was determined using one-way analysis of variance (ANOVA) or Kruskal–Wallis test and further tested with post hoc LSD or Mann–Whitney analysis using GraphPad Prism 5.01. A statistical comparison of dermal elastosis found in all groups was determined with chi-square, exact Fisher and Kolmogorov–Smirnov. *P*-value < 0.05 was considered as statistically significant, while *P*-value < 0.01 was considered as statistically very significant. All statistics were computed using SPSS 23.0 software for windows.

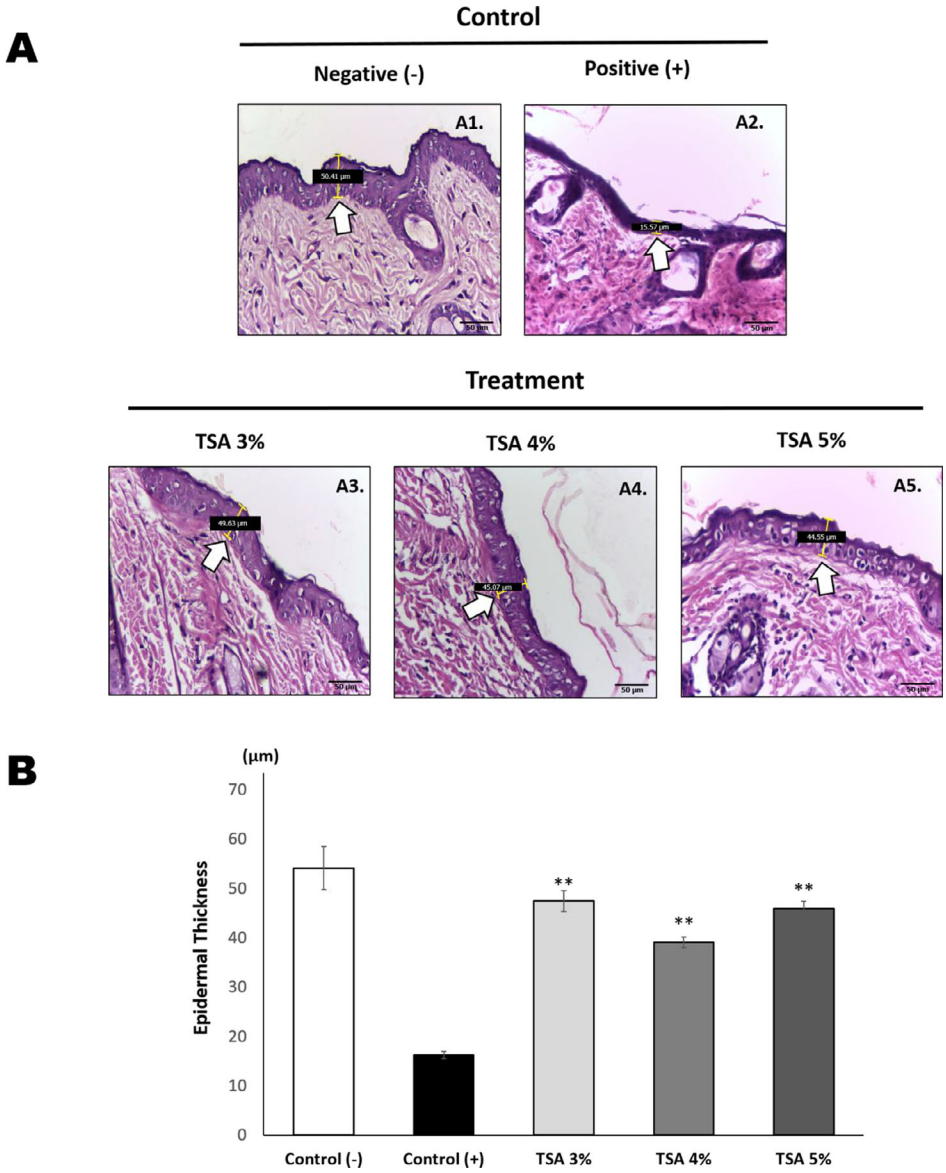

Figure 3. Evaluation of microscopic epidermal thickening following 10 weeks of UVB exposure with tranexamic acid treatment in mice skin with H&E staining. (A) Representative photomicrograph of epidermal thickness changes in all groups. [A1] No changes in epidermal thickness found in negative control group. [A2] There is a depletion of epidermal thickness found in positive control group. [A3-5] TSA cream application increased epidermal thickness in TSA 3%, 4% and 5% groups. (B) Significant increase in epidermal thickness was found in TSA 3%, 4% and 5% groups compared with positive control group. Data were presented as average mean ± standard error of mean (SEM) with $P < 0.05$ considered as significant (*) and $P < 0.01$ considered as very significant (**).

RESULTS

Macroscopic appearance

The physical examination showed variations among the groups which can be seen either macroscopically or manual palpation. On the negative group, it was observed the normal skin outlook and smooth. Whereas on the positive group, the wrinkled and rough skin outlook were observed. However, on the treatment group, improvement of the wrinkled skin was observed (Fig. 1).

Protein expression

Application of tranexamic acid cream increased protein expression levels of mitochondrial marker in mice skin. After 10 weeks of exposure to UVB and TSA cream application on mice skin,

Figure 4. Representative photomicrograph of dermal elastosis with different degrees evaluated in all groups. (A) Mild dermal elastosis was found in negative control and TSA 4% group. Moderate dermal elastosis was found in all treatment groups. Severe dermal elastosis was found in positive control group. (B) TSA cream 4% reduced dermal elastosis to a group not exposed to UVB light.

A

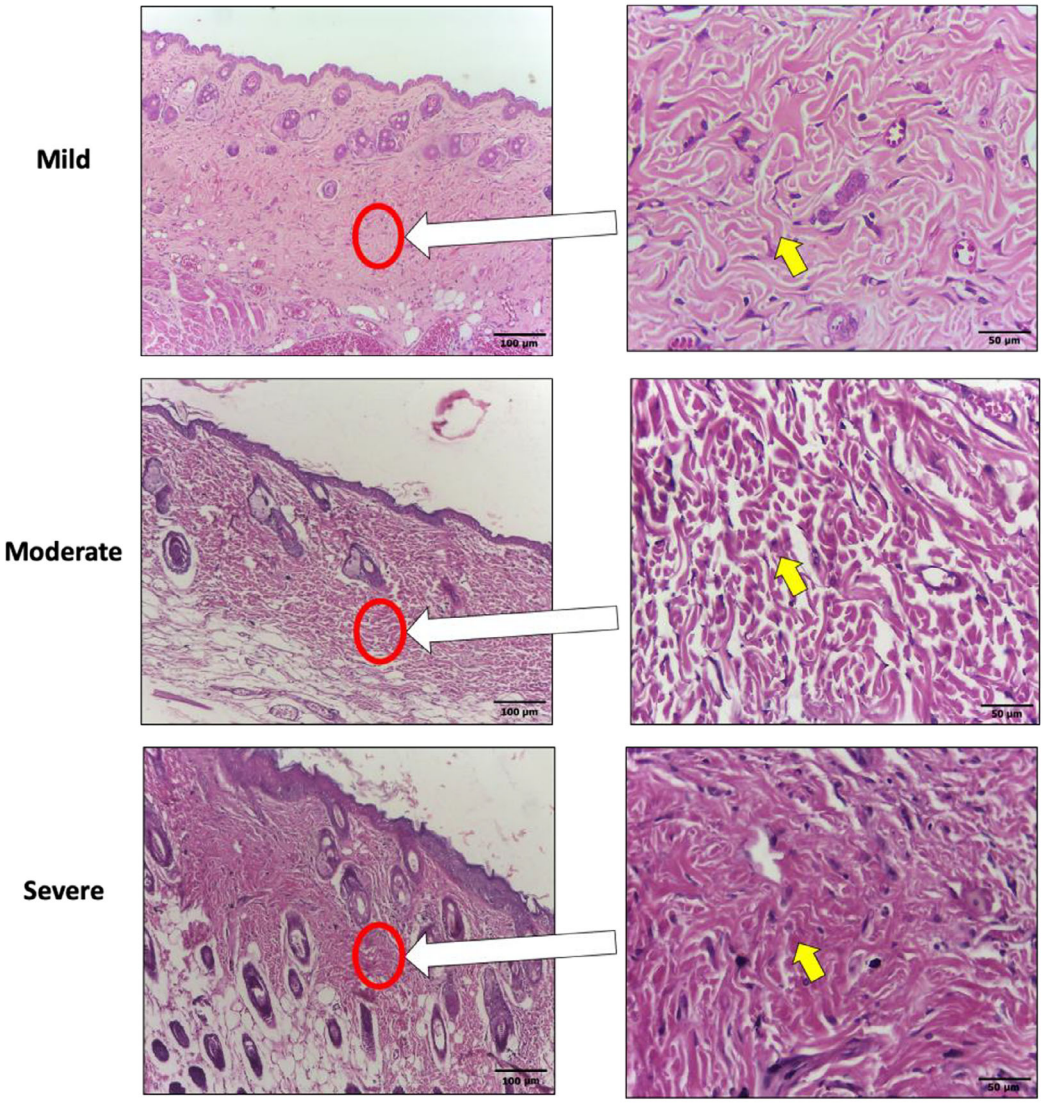

B

Variable	Degeneration of Dermal collagen fiber bundles (DCFB)			P Value
	Mild	Moderate	Severe	
Control (-)	100%	0%	0%	
Control (+)	0%	0%	100%	
TSA 3%	16.7%	72.2%	11.1%	0.0001**
TSA 4%	83.3%	16.7%	0%	
TSA 5%	0%	83.3%	16.7%	

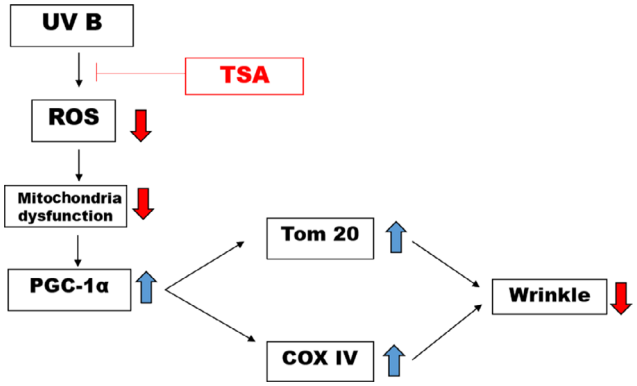

Figure 5. Proposed mechanism. UVB exposure increases the formation of ROS in the mice skin. Accumulation of ROS causes mitochondrial dysfunction, which is described by the decrease of mitochondrial markers. Mitochondrial dysfunction in the skin is characterized by the formation of wrinkles described by depletion of epidermal thickness and increased dermal elastosis. The administration of AT cream can improve wrinkles, and this is thought to be the improvement and regeneration of mitochondria seen from the increase in mitochondrial markers: PGC1α, Tom 20, COX IV and improvement of skin histology.

protein level of PGC1α was significantly increased in all TSA groups (1.4-fold for TSA 3%, 1.6-fold for TSA 4% and 1.7-fold for TSA 5%), while Tom20 was only significantly increased in TSA 5% group (1.7-fold for TSA 3%, 1.6-fold for TSA 4% and 2.5-fold for TSA 5%), and COXIV was significantly increased in TSA 3% and 5% groups (1.6-fold for TSA 3%, 1.3-fold for TSA 4% and 2.9-fold for TSA 5%), compared with positive control (Fig. 2B).

Histological changes

Tranexamic acid cream improved epidermal thickness and dermal elastosis. Hematoxylin- and eosin-stained sections from skin samples were analyzed for thickening of the epidermis and dermal elastosis. A significantly increased epidermal thickness (Fig. 3A) (2.92-fold for TSA 3%; 2.40-fold for TSA 4%; and 2.82-fold for TSA 5% group) (Fig. 3A,B) and reduction in the degree of dermal elastosis (16.7% for TSA 3%, 83.3% for TSA 4% group) (Fig. 4A,B) were found after application of TSA cream to negative controls.

DISCUSSION

Recently, TSA is widely used in antiaging products as antimelasma (23). Oral TSA administration in NOA type hairless mice (Naruto Research Institute Otsuka Atrichia) had been reported improved wrinkles by reducing transepidermal water loss (TEWL), increased skin hydration capacity, increased type I collagen levels and decreased matrix metalloproteinase-1 (MMP-1) levels. In addition, administration of oral TSA also increased β-endorphin levels, fibroblast cell proliferation and type I collagen production (21).

Wrinkles on the skin provide a histological picture of epidermal thinning, abnormal elastin tissue deposition in the dermal layer and hypodermic atrophy (24). Environmental factors such as air pollution, smoking history and chronic sun exposure exercise are considered important in wrinkles (25). The accumulation of UVB exposure caused loss of skin elasticity, which is one of the causes of wrinkles (26,27) (Fig. 1). In our study, we found that TSA cream could improve wrinkle repair by increasing epidermal thickness (Fig. 3 [A3-5]) and degeneration of dermal collagen fiber bundle lead to decrease in dermal elastosis (Fig. 4A, B) in mice skin exposed to UVB. UVB exposure increases ROS formation in the skin, and its accumulation causes mitochondrial dysfunction (28). Photoaging skin, which is characterized by wrinkles, is closely related to the reduction in mitochondrial function (29). Our study had showed that TSA treatment could abolish or at least partly reduce UV-induced mitochondrial damage which reflected from level PGC1α, Tom 20 and COX IV (Fig. 2). Therefore, improvement in the function and regeneration of mitochondria may be able to correct or improve the wrinkling process that occurs during aging (30). UVB exposure induces the decrease in mitochondrial marker levels, and by giving TSA cream 3%, 4% and 5%, the markers are observed to be increased (Fig. 2).

Taken together, our study had revealed that TSA cream had an effect as an antiwrinkle agent via control of mitochondrial biogenesis which influenced epidermal thickness and decreased degeneration of dermal collagen fiber bundle lead to dermal elastosis (Fig. 5). In summary, TSA cream application on the mice skin after exposure to UVB reduces epidermal thickness and dermal elastosis, while increasing mitochondrial marker levels of PGC1α, Tom20 and COX IV.

Acknowledgements—The authors would like to thank Susianti and Nurul Ihsani for technical assistance during experiments. This study was supported by funding granted from Indonesian Ministry of Research, Technology and Higher Education, PDUPT Scheme Grant Aid to RL Number: 3854/UNG.C/LT/2019.

SUPPORTING INFORMATION

Additional supporting information may be found online in the Supporting Information section at the end of the article:

Figure S1. Experimental design of the research.

Figure S2. Cage design for experiment.

REFERENCES

1. Krutmann, J. (2017) Skin aging: A brief summary of characteristic changes. In *Textbook of Aging Skin* (Edited by M. A. Farage, K. W. Miller and H. I. Maibach), pp. 55–66. Springer, Berlin.
2. Addor, F. A. S. (2018) Beyond photoaging : Additional factors involved in the process of skin aging. *Clin. Cosmet. Investig. Dermatol.* **11**, 437–443.
3. Lee, C.-H., S.-B. Wu, C.-H. Hong, H.-S. Yu and Y.-H. Wei (2013) Molecular mechanisms of uv-induced apoptosis and its effects on skin residential cells: the implication in uv-based phototherapy. *Int. J. Mol. Sci.* **14**, 6414–6435.
4. Bolisetty, S. and E. A. Jaimes (2013) Mitochondria and reactive oxygen species: Physiology and pathophysiology. *Int. J. Mol. Sci* **14**, 6306–6344.
5. Osellame, L. D., T. S. Blacker, M. R. Duchen and B. A. Oxon (2012) Cellular and molecular mechanisms of mitochondrial function. *Best Pract. Res. Clin. Endocrinol. Metab.* **26**, 711–723.
6. Naidoo, K., R. Hanna and M. A. Birch-machin (2017) What is the role of mitochondrial dysfunction in skin photoaging? *Exp. Dermatol.* **27**, 124–128.
7. Chistiakov, D. A., I. A. Sobenin, V. V. Revin, A. N. Orekhov and Y. V. Bobryshev (2014) Mitochondrial aging and age-related dysfunction of mitochondria. *Biomed. Res. Int.* **2014**, 1–7.

8. Krutmann, J. (2017) Pathomechanisms of photoaged skin. In *Textbook of Aging Skin* (Edited by M. A. Farage, K. W. Miller and H. I. Maibach), pp. 121–129. Springer, Berlin.
9. Stout, R. and M. Birch-machin (2019) Mitochondria's role in skin ageing. *Biology (Basel).* **8**, 29.
10. Sun, N., R. J. Youle and T. Finkel (2016) The mitochondrial basis of aging. *Mol. Cell.* **61**, 654–666.
11. Saki, M. and A. Prakash (2017) DNA damage related crosstalk between the nucleus and mitochondria. *Free Radic. Biol. Med.* **107**, 216–227.
12. Shokolenko, I., N. Venediktova, A. Bochkareva, G. L. Wilson and M. F. Alexeyev (2009) Oxidative stress induces degradation of mitochondrial DNA. *Nucleic Acids Res.* **37**, 2539–2548.
13. Gonzalez-freire, M., R. De Cabo, M. Bernier, S. J. Sollott, E. Fabbri, P. Navas and L. Ferrucci (2015) Reconsidering the role of mitochondria in aging. *J. Gerontol. A Biol. Sci. Med. Sci.* **70**, 1334–1342.
14. Barja, G. (2013) Updating the mitochondrial free radical theory of aging : and confounding concepts. *Antioxid. Redox Signal.* **19**, 1420–1445.
15. Wurm, C. A., D. Neumann, M. A. Lauterbach, B. Harke, A. Egner, S. W. Hell and S. Jakobs (2011) Nanoscale distribution of mitochondrial import receptor Tom20 is adjusted to cellular conditions and exhibits an inner-cellular gradient. *Proc. Natl. Acad. Sci. USA* **108**, 13546–13551.
16. Kish, S. J., C. Bergeron, A. Rajput, S. Dozic, F. Frank Mastrogiacomo, L.-J. Chan, J. M. Wilson, L. M. DiStefano and J. N. Nobrega (1992) Rapid communication brain cytochrome oxidase in Alzheimer's disease. *J. Neurochem.* **59**, 776–779.
17. Kligman, A. M. (1969) Early destructive effect of sunlight on human skin. *JAMA* **210**, 2377–2380.
18. Hughes, M. C., C. Bredoux, F. Salas, D. Lombard, G. M. Strutton, A. Fourtanier and A. C. Green (2011) Comparison of histological measures of skin photoaging. *Dermatology* **223**, 140–151.
19. Zhang, L., W. Tan, Q. Fang, W. Zhao, Q. Zhao, J. Gao and X. Wang (2018) Tranexamic acid for adults with melasma : a systematic review and meta-analysis. *Biomed. Res. Int.* **2018**, 1–13.
20. Na, J., S. Choi, S. Yang, H. Choi, H. Kang and K. Park (2013) Effect of tranexamic acid on melasma: A clinical trial with histological evaluation. *J. Eur. Acad. Dermatol. Venereol.* **27**, 1035–1039.
21. Hiramoto, K., D. Sugiyama, Y. Takahashi and E. Mafune (2016) The amelioration effect of tranexamic acid in wrinkles induced by skin dryness. *Biomed. Pharmacother.* **80**, 16–22.
22. Kawabata, K., M. Kobayashi, E. Akasaka, T. Mabuchi, T. Fukui, Y. Sugiyama, S. Takekoshi, M. Miyasaka, A. Ozawa and S. Sakai (2014) A new objective histological scale for studying human photoaged skin. *Ski. Res. Technol.* **20**, 155–163.
23. Grimes, P. E., S. Ijaz, R. Nashawati and D. Kwak (2019) New oral and topical approaches for the treatment of melasma. *Int. J. Womens Dermatol.* **5**, 30–36.
24. El-domyati, M., W. Medhat, H. M. Abdel-wahab and N. H. Moftah (2014) Forehead wrinkles: A histological and immunohistochemical evaluation. *J. Cosmet. Dermatol.* **13**, 188–194.
25. Farage, M. A., K. W. Miller and H. I. Maibach (2017) Degenerative changes in aging skin. In *Textbook of Aging Skin* (Edited by M. A. Farage, K. W. Miller and H. I. Maibach), pp. 15–27. Springer, Berlin.
26. Charoenchon, N., L. E. Rhodes, S. M. Pilkington, M. D. Farrar and R. E. B. Watson (2018) Differential reorganisation of cutaneous elastic fibres: A comparison of the in vivo effects of broadband ultraviolet B versus solar simulated radiation. *Photochem. Photobiol. Sci.* **17**, 889–895.
27. Dhital, B., P. Durlik, P. Rathod, F. Gul-e-noor, Z. Wang, C. Sun, E. J. Chang, B. Itin and G. S. Boutis (2017) Ultraviolet radiation reduces desmosine cross-links in elastin. *Biochem. Biophys. Rep.* **10**, 172–177.
28. Jugé, R., J. Breugnot, C. Da Silva, S. Bordes and B. Closs (2016) Quantification and characterization of uvb-induced mitochondrial fragmentation in normal primary human keratinocytes. *Nat. Publ. Gr.* **6**, 1–9.
29. Paz, M. L., D. H. G. Maglio, F. S. Weill, J. Bustamante and J. Leoni (2008) Mitochondrial dysfunction and cellular stress progression after ultraviolet B irradiation in human keratinocytes. *Photodermatol. Photoimmunol. Photomed.* **24**, 115–122.
30. Singh, B., T. R. Schoeb, P. Bajpai, A. Slominski and K. K. Singh (2018) Reversing wrinkled skin and hair loss in mice by restoring mitochondrial function. *Cell Death Dis.* **9**, 1–14.